arXiv:1602.07561v2 [quant-ph] 30 Dec 2016

The Quantum-Classical Boundary for Precision Interferometric Measurements

Patrick M. Birchall,* Jeremy L. O'Brien, Jonathan C. F. Matthews, and Hugo Cable†
Quantum Engineering Technology Labs, H. H. Wills Physics Laboratory and Department of Electrical and Electronic Engineering, University of Bristol, Merchant Venturers Building, Woodland Road, Bristol BS8 1FD, UK.
(Dated: December 30, 2016)

Understanding the fundamental limits on precision measurements of optical phase is of key interest for many investigative techniques utilized across science and technology. We study the measurement of an optical phase shift, which has an associated optical loss, and compare measurement strategies using classical and non-classical probe states. We find that, for a given number of incident photons upon the unknown phase, non-classical techniques provide less than a 20% reduction in root-mean-square-error (RMSE) in comparison with classical techniques in multi-pass optical setups. Using classical techniques in a new optical setup we devise, the achievable reduction in RMSE afforded by non-classical techniques falls to only $\simeq 4\%$.

The use of non-classical techniques to perform high-precision measurements is the subject of intensive research efforts [1]. The applications of high-precision interferometry are widespread, and are subject to different limiting factors. An early quantum-enhanced strategy for gravitational wave detection was proposed in 1980 using optical interferometry [2]. By considering the limitations placed on the system by the total power available, radiation-pressure-induced dephasing and optical loss, it was shown that squeezed states could be used to increase sensitivity.

In many subsequent treatments of interferometric quantum metrology, many practical factors were set aside, and the focus was abstracted to estimating a phase (in one mode) encoded in a state by a unitary operator $|\psi(\theta)\rangle = \exp(\mathrm{i}\hat{n}_1\theta)|\psi(0)\rangle$ [3]. The typical figure of merit was the obtainable precision and how this scales with the number of photons used $\Delta\theta = g(N)$ [4]. Once dephasing and loss have been omitted, the best choice of input state for detecting small phase shifts is the N00N state $|N,0\rangle_{1,2} + |0,N\rangle_{1,2}$ [5]. The use of non-classical input states allows measurement uncertainty to be reduced from the standard quantum limit (SQL) $\Delta\theta = 1/\sqrt{N}$ to $\Delta\theta = 1/N$, known as the Heisenberg limit [6]. However this reduction in uncertainty should be understood within the context of the assumptions used to derive it. For example, if one is concerned with measuring a fixed phase, instead of a time-varying one, then this increase in precision beyond the SQL can be achieved using classical states by increasing the number of times the phase shift is applied to each photon using multi-pass (MP) strategies; as depicted in Fig. 1a) [7]. Furthermore, if there is any optical loss the measurement uncertainty scaling is proportional to the SQL and the quadratic improvement is lost [8, 9].

In this letter we study measurement of an optical phase shift which remains fixed in time, where optical loss is the dominant non-ideal process, focusing on the precision one can achieve whilst passing a limited number of photons through the phase-shift. This situation affords the opportunity for a truly non-classical advantage which cannot be emulated by increased laser power. Performing high precision measurements using low levels of incident energy is necessary to perform measurements of biological and other delicate systems [11]. First we will compare the properties of N00N state and classical MP strategies, as well as optimal classical MP and optimal quantum strategies [8, 9]. In search of practical quantum strategies, we then look at how well one can do with Gaussian states and intensity measurements. We will also consider classical input states in more general optical setups, to assess further scope for increased precision afforded by non-classical techniques.

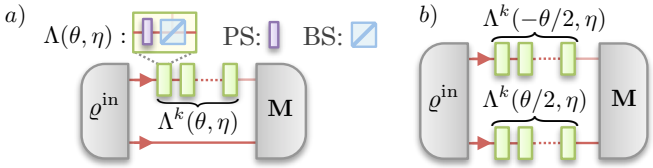

FIG. 1. MP schemes using an input state ϱ^{in} and k passes through the lossy phase-shift (PS), $\Lambda(\theta,\eta)$, before measurement with a positive-operator value measure (POVM). $a)$ An absorptive or lossy optical phase $\Lambda(\theta,\eta)$ can be described by a beam-splitter (BS), of transmissivity η, coupling into a vacuous environment mode and a unitary phase-shift of θ: $\mathrm{e}^{\mathrm{i}\hat{n}\theta}$. To measure a lossy phase shift in one mode, a MP strategy can be used together with a reference beam. $b)$ To measure a phase difference between two modes, equal and opposite phase shifts are considered here acting on each mode [10].

To assess the precision capabilities of different schemes we use the quantum Fisher information (QFI) [12, 13]. Once a parameter has been encoded onto a quantum state $\varrho_\theta = \sum_i p_i(\theta)|\psi_i(\theta)\rangle\langle\psi_i(\theta)|$, expressed in terms of the eigenvectors of ϱ_θ, the QFI is defined as $F(\varrho_\theta) \equiv \mathrm{tr}\left[\varrho_\theta \mathcal{L}_\theta^2(\varrho_\theta)\right]$, where $\mathcal{L}_\theta(\varrho_\theta) = \sum_{i,j} 2\langle\psi_i|\frac{\partial}{\partial\theta}\varrho_\theta|\psi_j\rangle|\psi_i\rangle\langle\psi_j|/(p_i+p_j)$ is the symmetric logarithmic derivative (SLD). $F(\varrho_\theta)$ bounds the precision to which θ can be estimated through the quantum Cramér-Rao bound:

$$F(\varrho_\theta) \equiv \mathrm{tr}\left[\varrho_\theta \mathcal{L}_\theta^2(\varrho_\theta)\right] \geq 1/\Delta^2\theta, \tag{1}$$

where $\Delta^2\theta$ is the mean-square error of unbiased estimates of θ. Thus QFI provides a measurement-basis independent evaluation of ϱ_θ. Given a non-optimal measurement by a POVM, $\mathbf{M}$, the regular Cramér-Rao inequality provides a tighter bound on precision: $F_{\mathbf{M}}(\varrho_\theta) \geq 1/\Delta^2\theta$, where $F_{\mathbf{M}}$ is a function of all the probabilities of possible measurement outcomes [14]. By considering the input state and the setup used to encode the phase, we can make a full accounting of

the resources required to achieve a given precision.

We turn now to the example of a N00N state probing a two-mode (TM) lossy phase, as in Fig. 1b). An N-photon N00N state which has passed through a TM lossy phase once achieves QFI equal to that for coherent states, with total mean photon number of one and equal intensity in each mode, when passed through a TM lossy phase N times [15, 16]. However, the mean number of photons which pass through the phase shift are not equal in both cases. For the N00N state all N photons are incident upon the phase shift. For the coherent states, the mean number of photons decreases with each pass, and the number of times each photon passes through the phase shift is always less than N, for $N > 1$ (see appendix A). Thus, by passing the coherent state through the phase N times, the phase will absorb fewer photons than if a N00N state had been used. We therefore conclude that NOON states are actually sub-classical resources for the task we are considering. Note that other works have considered the number of particles in the probe multiplied by the number of passes through the phase shift, for which N00N states are equivalent to classical MP strategies [15–17]; using this equivalence and by studying the capabilities of all definite photon number states it was found that, for a given N, using quantum states instead of classical strategies could provide a reduction in RMSE of at most $\sim 39.3\%$ for all values of η [17].

NOON states have been shown to be among the most fragile states, losing all their phase sensing capability when any number of the photons are lost. Therefore in order to find the scope for a quantum advantage, we compare classical strategies to upper bounds on the phase sensing abilities of any quantum state in the presence of loss.

Classical multi-pass strategies: Next we consider the case where there is no reference beam, depicted in Fig. 1b), which has been studied extensively in the literature. The actions of phase, θ, and loss, $(1-\eta)$, commute [18] and therefore, in the ideal case when no additional loss is encountered between each application of the channel, k applications of the channel $\Lambda^k(\eta,\theta)[\bullet] \equiv \Lambda(\eta,\theta)[\Lambda(\eta,\theta)[\cdots\Lambda(\eta,\theta)[\bullet]\cdots]]$ perform the same operation as $\Lambda(\eta^k, k\,\theta)$, where here and throughout η and θ are quantities intrinsic to each single application of a lossy-phase. Hence known results from single-pass (SP) strategies can be easily modified for the MP case. The figure of merit we maximize is the QFI per average total number of lost photons, which will be denoted as F'. This is equivalent to maximizing the QFI per incident photon for some intrinsic transmissivity, as the average total number lost at the lossy-phase $\langle\hat{n}_l\rangle$ over all interrogations, and the total number incident $\langle\hat{n}_i\rangle$, are related by $\langle\hat{n}_l\rangle = \langle\hat{n}_i\rangle(1-\eta)$ and consequently either $\langle\hat{n}_l\rangle$ or $\langle\hat{n}_i\rangle$ may be considered the resource whose use we are minimizing. Therefore F' using k passes through the phase shift will be:

$$F'(\varrho^{\text{out}}, k) = F(\varrho^{\text{out}}, k)\big/\big[\operatorname{tr}(\hat{N}\varrho^{\text{in}})(1-\eta^k)\big]. \tag{2}$$

where $\hat{N}$ is the total number of photons within a state. For any k and η, the classical (coherent) input state which maximizes $F(\varrho^{\text{out}}, k)$, where $\varrho^{\text{out}} = \Lambda(\eta^k, k\theta)[\varrho^{\text{in}}]$, is the TM coherent state $\varrho^{\text{in}}_{\text{Cl}} = |\alpha/\sqrt{2}, \alpha/\sqrt{2}\rangle$ with $\operatorname{tr}(\hat{N}\varrho^{\text{in}}) = |\alpha|^2$. Here $F(\varrho^{\text{out}}_{\text{Cl}}, k) = \operatorname{tr}(\hat{N}\varrho^{\text{in}})\eta^k k^2$, and hence:

$$F'(\varrho^{\text{out}}_{\text{Cl}}, k) = \eta^k k^2/(1-\eta^k), \tag{3}$$

which is independent of $|\alpha|^2$. MP schemes benefit from a factor of k^2 in the QFI as the phase shift is magnified coherently by k. As $\Delta^2\theta = \Delta^2(k\tilde{\theta}) \implies \Delta^2\theta/k^2 = \Delta^2\tilde{\theta}$ (which shows the mean-squared error (MSE) is reduced by a factor of k^2). At the same time the total transmissivity is also reduced exponentially becoming η^k.

In order to find an analytic solution for the optimal number of passes we permit k to be non-integer. Doing so we find $F'(\varrho^{\text{out}}_{\text{Cl}}, k)$ is optimized when: $k_{\text{opt}} = -(2+\mathcal{W})/\ln(\eta) \approx -1.59/\ln(\eta)$, where $\mathcal{W} \equiv W_0(-2/\text{e}^2) \approx -0.406$ is the main branch of the Lambert W function at $-2/\text{e}^2$ [19]. This solution for k keeps the overall proportion of light transmitted constant $\eta^{k_{\text{opt}}} \approx 20.32\%$. Counterintuitively, we have found that in order to lose as few photons overall, it is best for the lossy phase to lose $\sim 80\%$ of the total input light. In which case,

$$F'(\varrho^{\text{out}}_{\text{Cl}}, k_{\text{opt}}) = -\mathcal{W}(2+\mathcal{W})/\ln^2(\eta) \approx 0.648/\ln^2(\eta). \tag{4}$$

For comparison, the QFI for a single-pass (SP) strategy is bounded above, for any input state ϱ^{in} and transmissivity, by [8, 9, 20]:

$$Q_{\text{TM}} \equiv \operatorname{tr}(\hat{N}\varrho^{\text{in}})\eta/(1-\eta) \geq F(\varrho^{\text{out}}) \tag{5}$$

in a two-mode (TM) setup as in Fig. 1b). This bound is asymptotically saturable for large $\operatorname{tr}(\hat{N}\varrho^{\text{in}})$, leading to a saturable bound on the QFI per lost photon of: $Q'_{\text{TM}} = \eta/(1-\eta)^2$. For MP strategies the bound becomes: $Q'_{\text{TM}}(k) = \eta^k k^2/(1-\eta^k)^2$ as described in Appendix B. Permitting k to be continuous to allow for a fair comparison with the classical strategy, the previous expression is maximized in the limit: $\lim_{k\to 0} Q'_{\text{TM}}(k) = 1/\ln^2(\eta)$. Therefore, we find the ratio of achievable precisions for a given mean number of incident photons to be:

$$\frac{\Delta\theta_{\text{Q}}}{\Delta\theta_{\text{Cl}}} = \sqrt{\frac{F'(\varrho^{\text{out}}_{\text{Cl}}, k_{\text{opt}})}{\lim_{k\to 0} Q'_{\text{TM}}(k)}} \approx 0.805, \tag{6}$$

i.e. the reduction in root-MSE (RMSE) afforded by non-classical input states over classical MP strategies is $\sim 19.5\%$.

If instead the lossy phase is confined to a single mode (SM), as in Fig. 1a), then a reference beam can provide additional precision. The optimal classical state will then comprise two coherent states $\varrho_{\text{Cl}} = |\alpha, \beta\rangle$ where $|\beta|$ is very large. In this situation F' can be calculated as above to be four times larger than the expression given in Eq. (3), and is maximized for the same value of k. Quantum strategies can also benefit from a reference beam. In this case the bound on quantum strategies is four times larger than given in Eq. (13), and the mean number of photons in the input state $\operatorname{tr}(\hat{N}\varrho^{\text{in}})$ is replaced by those which are incident upon the lossy phase, $\langle\hat{n}_i\rangle$,

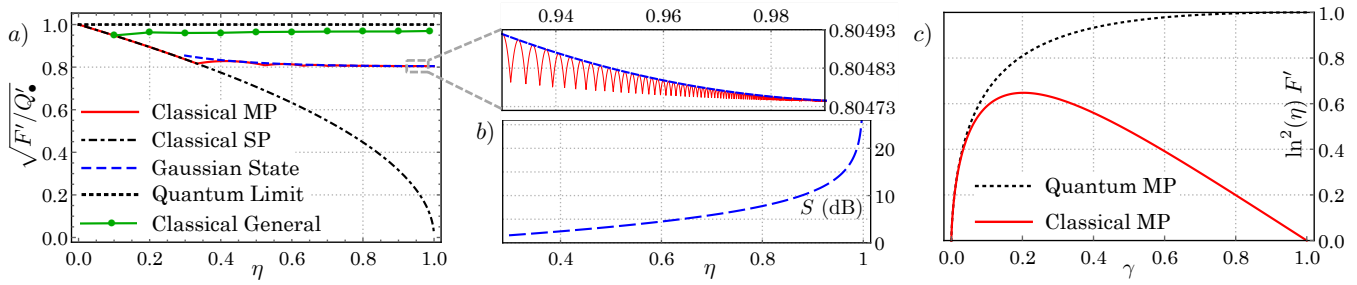

FIG. 2. *a*) The achievable precisions $1/\Delta\theta = \sqrt{lF'(\varrho)}$ for all the schemes discussed when a discrete number of interrogations is used, normalized to the relevant SM or TM quantum limit on precision $1/\Delta\theta_Q = \sqrt{lQ'_\bullet}$, $\bullet$ = SM or TM for an equal mean number of lost photons, l. The inset shows bumps each corresponding to a different integer k. *b*) Squeezing, in dB, required for the phase-squeezed Gaussian state shown in the left most plot. *c*) F' for classical or optimal quantum states when interrogating a phase with a transmissivity of η in a MP configuration. Classical-MP strategies require lower overall transmission, $\gamma = \eta^k$, to perform well. The classical MP curve remains relatively flat near the optimal γ, hence k does not need to be set precisely for a classical MP scheme to perform well.

giving a revised quantum bound on the QFI per lost photon, $Q_{\text{SM}} = 4\langle\hat{n}_i\rangle\eta/(1-\eta)$ [9], and associated optimal MP QFI per lost photon for continuous k:

$$\lim_{k\to 0} Q'_{\text{SM}}(k) = 4/\ln^2(\eta). \tag{7}$$

The ratio between quantum and classical strategies remains unchanged. As stated in Ref. [9] this revised bound for SM phase estimation, Q_{SM}, has tremendous universality, and holds even when arbitrary operations are performed between interrogations of the phase. It too is saturable in the large $\langle n_i\rangle$ limit e.g. a highly squeezed-vacuum input state [21].

When measuring the phase shift imparted by a gas or a liquid medium, the length of the sample, corresponding to a choice of k, may be chosen from a continuum of values; however if the system under investigation is intrinsically discrete then k must be an integer to reflect this. Restricting k_{opt} to be an integer number of passes alters the ratio in Eq. (6). The effect of this restriction is plotted in Fig. 2a) and shows that the reduction in RMSE granted by non-classical techniques remains less than 20% for any value of η when a discrete number of passes must be used.

Optimal strategies: So far it has been shown that the optimal number of passes for both quantum and classical input states result in a fixed amount of loss. In fact, we will now argue that this is true for more general optical setups, in which are embedded h multi-pass modules of k lossy phases, each followed by an adaptive control phase ϕ. Any network with h modules will be a quantum channel of the form: $\mathcal{E}_h\{\Lambda(\eta^k, k\theta+\phi)[\cdots\mathcal{E}_1\{\Lambda(\eta^k, k\theta+\phi)[\bullet]\}\cdots]\}$ where $\mathcal{E}_i\{\bullet\}$ describes an arbitrary quantum channel enacted by the optical setup (between the i^{th} and $i+1^{\text{th}}$ multi-pass modules). This network will produce an output state, $\varrho(\eta^k, k\theta+\phi) = \sum_i p_i|\psi_i\rangle\langle\psi_i|$ where all the terms may depend on η^k and $k\theta+\phi$, for which

$$\begin{aligned} F'\left[\varrho(k\theta+\phi,\eta^k)\right] &= \text{tr}\left[\varrho\mathcal{L}^2_\theta(\varrho)\right] / \text{tr}\left[\hat{N}(\varrho-\varrho^{\text{in}})\right], \\ \mathcal{L}_\theta(\varrho) &= k\textstyle\sum_{i,j} 2\langle\psi_i|\frac{\partial}{\partial k\theta+\phi}(\varrho)|\psi_j\rangle|\psi_i\rangle\langle\psi_j|/(p_i+p_j). \end{aligned} \tag{8}$$

$\mathcal{L}_\theta(\varrho)$, is therefore a function of k, $k\theta+\phi$ and η^k such that the QFI per lost photon is of the form $F'(\varrho) = k^2 f(k\theta+\phi, \eta^k)$ for some function f. Re-parameterizing: $\eta^k = \gamma$ and $k\theta+\phi = \varphi$ we see that $k = \ln\gamma/\ln\eta$ and:

$$F'(\varrho) = \ln^{-2}\eta\,[\ln^2\gamma\, f(\varphi,\gamma)]. \tag{9}$$

Thus optimizing $F'(\varrho)$ over k and ϕ for all values of η and θ correspond to optimizing $\ln^2\gamma\, f(\varphi,\gamma)$ over φ and γ. From Eq.'s (8) and (9) we conclude that, whilst F' may have very complex dependence on φ, γ and each $\mathcal{E}_i$, for any setup comprised of h multi-pass modules the following statement always applies: the phase encoding should be adjusted to produce the same output state independently of the loss encountered with each individual pass of the state through the channel, i.e. there is an optimal amount of total loss that the state should undergo. We note that all setups, in which there is at least a single pass though a lossy phase, can be considered to contain a multi-pass module with a k of at least one. If k is restricted to be an integer then it will not always be possible to achieve a desired amount of loss and the strategy will be degraded in comparison with the optimal continuous k strategy. This will be more significant when η is small and there is little freedom to choose how much light is lost.

Note that when there is no prior information about θ, φ cannot initially be controlled to a high precision. As subsequent probe states are sent through an optical network and then measured, information about θ is gained and the precision to which φ can be set by adjusting ϕ will improve. This ensures that the procedure obtains measurement outcomes which are highly sensitive to θ. Over many repetitions of the measurement, the fraction of information gained using a significantly suboptimal value for φ can be continually reduced. As the QFI, for all of the strategies discussed, grows proportional to the number of input photons in each input-state this requirement for many repetitions will not reduce the performance of these strategies when the total number of photons used is large. In the limit of $\eta \to 1$ our analysis breaks down since the optimal number of passes will tend to infinity. Evaluating the merit of different strategies when $\eta = 1$ requires a Bayesian analysis [22] and we note that, in this limit no incident power

is absorbed and therefore the absorbed power cannot damage the sample under investigation.

Applying the parameterization $\gamma = \eta^k$, used to find Eq. (9), the FI per incident photon of the classical- and quantum-MP strategies can be compared as a function of γ as shown in Fig. 2c). A comparison of the RMSEs associated with the classical- and quantum-MP strategies corresponds to the square root of lines in Fig. 2c). This plot shows that, whilst classical-MP strategies require $\gamma = \eta^{k_{\text{opt}}} \simeq 20.32\%$ to perform optimally, the classical MP curve remains relatively flat near k_{opt} hence k only needs to be set such that γ is near $20.32 \pm 10\%$.

Gaussian-state strategy: For SP-TM phase estimation, with balanced loss in each of the two modes, the problem of maximizing precision whilst passing a given mean number of photons through the sample is equivalent to maximizing precision for a fixed mean number of photons in the input state. This is a task which as been investigated thoroughly [15, 18, 23–25] and it has been shown that for TM lossy phase estimation, the Gaussian state suggested in [2] coupled with intensity measurements saturates the ultimate limit on precision given in Eq. (13) [2, 20]. This state is implemented in GEO600 an interferometer for gravitational wave detection [26–28]. However, for both SM phase estimation and TM phase estimation with unbalanced loss: considering the resource to be the number of lost photons demands distinctly different solutions to those found by minimizing the total number of photons in an optical state (including any required reference beam). In light of this important distinction, we evaluate the potential for practical gains using non-classical states for SM phase estimation with SM Gaussian input states and homodyne detection due to their relative experimental simplicity.

SM Gaussian states are fully characterized by a displacement vector $\boldsymbol{d}$ of means, $d_i = \langle \hat{x}_i \rangle$, and matrix $\boldsymbol{\Gamma}$ of covariances, $\Gamma_{ij} = \frac{1}{2}\langle \hat{x}_i \hat{x}_j + \hat{x}_j \hat{x}_i \rangle - \langle \hat{x}_i \rangle \langle \hat{x}_j \rangle$, of the quadrature operators $\hat{x}_1 = \frac{1}{2}(\hat{a}^\dagger + \hat{a})$ and $\hat{x}_2 = \frac{1}{2} i (\hat{a}^\dagger - \hat{a})$ [29]. Homodyne measurement of the SM state can be performed using a reference beam, to enact a measurement of the $\hat{x}_1$ quadrature [29]. An arbitrary SM pure Gaussian state can be defined by the squeezing $\hat{S}(r,\phi) = \exp[\frac{1}{2} r(\mathrm{e}^{\mathrm{i}\phi}\hat{a}^2 - \mathrm{e}^{-\mathrm{i}\phi}\hat{a}^{\dagger 2})]$, displacement $\hat{D}(\alpha) = \exp[\alpha(\hat{a}^\dagger - \hat{a})]$, and rotation $\hat{R}(\varphi) = \exp(\mathrm{i}\hat{a}^\dagger \hat{a}\, \varphi)$ operators acting on a vacuum state: $\hat{R}(\varphi)\hat{D}(\alpha)\hat{S}(r,\phi)|0\rangle$ where all arguments are real and the mean number of photons is: $\langle \hat{N} \rangle = \alpha^2 + \sinh^2(r)$. We investigate phase-squeezed coherent states, $\phi = \pi$, and evaluate the Fisher information of the output state, $\varrho_{\text{G}}^{\text{out}}$, at the homodyne angle $\varphi = \pi/2 - \theta$:

$$F_{\hat{x}}(\varrho_{\text{G}}^{\text{out}})\big|_{\varphi=\pi/2-\theta} = 4\alpha^2\eta \big/ \left[1 + (e^{-2r} - 1)\eta\right], \qquad (10)$$

see appendix C for details. When the number of photons contributing to the initial squeezing $n_{\text{sq}} = \sinh^2(r)$ is fixed but the total number of input photons is large, this scheme achieves a Fisher information per lost photon of:

$$\lim_{\langle \hat{N} \rangle \to \infty} F'_{\hat{x}}(\varrho_{\text{G}}^{\text{out}}) = \frac{1-\eta}{2\eta n_{\text{sq}} - 2\eta\sqrt{n_{\text{sq}}(n_{\text{sq}}+1)} + 1} \frac{4\eta}{(1-\eta)^2}. \qquad (11)$$

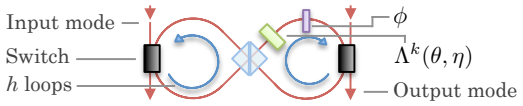

FIG. 3. A setup which interrogates an absorbing phase shift h times, with interference between each interrogation.

The quantum bound, Q'_{SM}, has been factorized here, to show that for a fixed n_{sq} and a given value of η a constant fraction of Q'_{SM} can be achieved for a large total number of photons. Eq. (11) saturates Q'_{SM} for large n_{sq}. We use this expression to find the amount of squeezing in dB, $S = 20r/\ln(10)$, needed to gain as much Fisher information per lost photon as the the optimal SM classical MP strategy which is given by four times the expression in Eq. (4). This is plotted in Fig. 2b).

Improved classical strategies: Next we ask if classical-MP strategies, which contain a single multi-pass module, can be surpassed by more complicated classical strategies. We consider the interrogation of a SM lossy phase embedded in a setup, such that between each interrogation interference occurs between the outgoing mode from the phase and another optical mode as shown in Fig. 3. Full details are provided in appendix D. We performed a heuristic optimization of the QFI per lost photon produced by this strategy for a series of values of $\eta = 0.1, 0.2 ... 0.9$ and found that: The optimal precision per incident photon exceeds the classical MP strategy, further reducing the scope for quantum enhancement to an average reduction in RMSE of 3.6% over this range of η. Individual results are plotted in Fig. 2a). Optimization details can be found in appendix E, and as the optimizations are not exhaustive there may be further room for improvement. Using additional reference beams, the same improvement can be made for TM phase estimation (as discussed in appendix F).

By carefully considering resources, the differences between ideal classical and ideal quantum strategies have been investigated to illuminate any fundamental advantage only obtainable through non-classical techniques. This is also instructive for practical situations when the dominant non-ideal effect is optical loss encountered at the lossy-phase; as technology improves over time this regime will extend to lossy phases with ever higher transmissivities. In appendix G we analyze a non-ideal multi-pass setup which has additional reduced transmissivities η_p, η_r and η_m associated with state-preparation, each single round-trip between applications of the lossy phase and the measurement stage respectively. We establish that if the round-trip loss is less than the combined state preparation and measurement loss ($\eta_r \geq \eta_p\eta_m$), the scope for reduced RMSE from non-classical techniques remains below 20%. This regime ($\eta_r \geq \eta_p\eta_m$) is practically relevant, applying to GEO600 where $\eta_p\eta_m \simeq 0.44$ [28], since low loss ($\leq 10^{-4}$) [30] passive optical elements can often be used to guide the light back to the lossy phase, whereas state-preparation and measurement require more complex and presently less efficient components such as non-linear crystals, filters and photodetectors. Conversely if $\eta_p\eta_m\eta \simeq 1$ and

$\eta_r \ll 1$, then quantum strategies would operate near ideally whilst classical strategies will not perform comparably, as using a large k is effectively prohibited by high round-trip loss. The performance of the improved classical strategy will be more heavily degraded by imperfect components due to its increased complexity which may nullify any precision gains.

In conclusion, we have found that for a given number of incident photons, the precision increase one can achieve for measuring fixed optical phase by using non-classical techniques is small. By explicitly considering resources we also noted that SM phase estimation requires different strategies, and thus provided a practical quantum strategy based on Gaussian states. This practical quantum strategy could be used for the measurement of a phase which is rapidly varying in time, since the classical techniques discussed in this work could suffer from blurring of temporal features due to increased interrogation time. In this situation there remains a large discrepancy between the achievable precision using classical and non-classical techniques.

Acknowledgments: We would like to thank D. Mahler for helpful comments on this manuscript. This work was supported by EPSRC, ERC, PICQUE, BBOI, US Army Research Office (ARO) Grant No. W911NF-14-1-0133, U.S. Air Force Office of Scientific Research (AFOSR) and the Centre for Nanoscience and Quantum Information (NSQI). J.L.O'B. acknowledges a Royal Society Wolfson Merit Award and a Royal Academy of Engineering Chair in Emerging Technologies. J.C.F.M. and J.L.O'B acknowledge fellowship support from the Engineering and Physical Sciences Research Council (EPSRC, UK).

* P.Birchall@Bristol.ac.uk
† Hugo.Cable@Bristol.ac.uk

[1] V. Giovannetti, S. Lloyd, and L. Maccone, Nature Photon. **5**, 222 (2011).
[2] C. M. Caves, Phys. Rev. D. **23**, 1693 (1981).
[3] V. Giovannetti, S. Lloyd, and L. Maccone, Science **306**, 1330 (2004).
[4] M. J. Holland and K. Burnett, Phys. Rev. Lett. **71**, 1355 (1993).
[5] J. P. Dowling, Contemp. Phys. **49**, 125 (2008).
[6] W. Heitler, *The quantum theory of radiation*, Vol. 86 (Courier Corporation, 1954).
[7] B. L. Higgins, D. W. Berry, S. D. Bartlett, H. M. Wiseman, and G. J. Pryde, Nature **450**, 393 (2007).
[8] S. Knysh, V. N. Smelyanskiy, and G. A. Durkin, Phys. Rev. A **83**, 021804 (2011).
[9] B. M. Escher, R. L. de Matos Filho, and L. Davidovich, Nature Phys. **7**, 406 (2011).
[10] M. Jarzyna and R. Demkowicz-Dobrzański, Phys. Rev. A **85**, 011801 (2012).
[11] M. A. Taylor and W. P. Bowen, Phys. Rep. **615**, 1 (2016).
[12] C. W. Helstrom, *Quantum detection and estimation theory* (Academic press, 1976).
[13] S. L. Braunstein and C. M. Caves, Phys. Rev. Lett. **72**, 3439 (1994).
[14] A. W. Van der Vaart, *Asymptotic statistics*, Vol. 3 (Cambridge university press, 2000).
[15] U. Dorner, R. Demkowicz-Dobrzanski, B. J. Smith, J. S. Lundeen, W. Wasilewski, K. Banaszek, and I. A. Walmsley, Phys. Rev. Lett. **102**, 040403 (2009).
[16] R. Demkowicz-Dobrzański, Laser Phys. **20**, 1197 (2010).
[17] R. Demkowicz-Dobrzański and L. Maccone, Phys. Rev. Lett. **113**, 250801 (2014).
[18] R. Demkowicz-Dobrzanski, U. Dorner, B. J. Smith, J. S. Lundeen, W. Wasilewski, K. Banaszek, and I. A. Walmsley, Phys. Rev. A **80**, 013825 (2009).
[19] R. M. Corless, G. H. Gonnet, D. E. Hare, D. J. Jeffrey, and D. E. Knuth, Adv. Comput. Math. **5**, 329 (1996).
[20] R. Demkowicz-Dobrzański, K. Banaszek, and R. Schnabel, Phys. Rev. A **88**, 041802 (2013).
[21] M. Aspachs, J. Calsamiglia, R. Munoz-Tapia, and E. Bagan, Phys. Rev. A **79**, 033834 (2009).
[22] D. W. Berry, B. L. Higgins, S. D. Bartlett, M. W. Mitchell, G. J. Pryde, and H. M. Wiseman, Phys. Rev. A **80**, 052114 (2009).
[23] M. Kacprowicz, R. Demkowicz-Dobrzański, W. Wasilewski, K. Banaszek, and I. A. Walmsley, Nature Photon. **4**, 357 (2010).
[24] N. Thomas-Peter, B. J. Smith, A. Datta, L. Zhang, U. Dorner, and I. A. Walmsley, Phys. Rev. Lett. **107**, 113603 (2011).
[25] H. Cable and G. A. Durkin, Phys. Rev. Lett. **105**, 013603 (2010).
[26] L. S. Collaboration *et al.*, Nature Phys. **7**, 962 (2011).
[27] H. Grote, K. Danzmann, K. L. Dooley, R. Schnabel, J. Slutsky, and H. Vahlbruch, Phys. Rev. Lett. **110**, 181101 (2013).
[28] J. Aasi, J. Abadie, B. P. Abbott, R. Abbott, T. D. Abbott, M. R. Abernathy, C. Adams, T. Adams, P. Addesso, R. X. Adhikari, *et al.*, Nature Photon. **7**, 613 (2013).
[29] R. Loudon and P. L. Knight, J. Mod. Opt. **34**, 709 (1987).
[30] For example, commercially available Semrock High-reflectivity Mirrors.
[31] O. Pinel, P. Jian, N. Treps, C. Fabre, and D. Braun, Phys. Rev. A **88**, 040102 (2013).
[32] G. Grimmett and D. Stirzaker, *Probability and random processes* (Oxford university press, 2001).

APPENDICES

A: N00N states vs. classical multi-pass

Here we calculate the number of incident photons, upon a TM lossy phase, when a the coherent state $|\alpha/\sqrt{2}\rangle|\alpha/\sqrt{2}\rangle$, with a mean photon number of $|\alpha|^2 = 1$, is passed through the TM lossy phase N times. The number of photons within the state will be reduced by a factor of η each time it passes through the lossy phase, such that the average total number of incident photons will be:

$$\sum_{p=1}^{N} \eta^{p-1}. \tag{12}$$

For $\eta < 1$ and $N > 1$ the above expression is less than N. The number of photons incident upon the lossy phase when an N photon N00N state is passed through it once is precisely N. Therefore, since the QFI of these two output states are equal, the QFI per incident photons is lower for the N00N state in comparison with a comparable classical MP strategy.

B: Multipass quantum limits

Here we discuss the multi-pass versions of the bounds on QFI. As stated in the main text: the upper bound on QFI per lost photon for TM phase estimation using any input state is [9]:

$$Q_{\rm TM} \equiv {\rm tr}(\hat{N}\varrho^{\rm in})\eta/(1-\eta) \geq F(\varrho^{\rm out}). \tag{13}$$

in the derivation of this equation η refers to the total transmissivity that the probe state experiences and bounds the QFI associated with the total phase shift experienced by the probe state. in the multi-pass case the transmissivitiy is instead η^k and so η^k replaces all occurrences of η to adapt this equation to the multi-pass case. in addition to the reduced transmissivity, the total phase shift is also magnified by a factor of k. The RMSE of estimates of this total phase shift $k\theta$ are bound by the limit on QFI with the reduced transmissivity: ${\rm tr}(\hat{N}\varrho^{\rm in})\eta^k/(1-\eta^k)$. This implies a limit on the estimation precision of θ by the following argument: since $\Delta^2(k\theta) = (1/k^2)\Delta^2\theta$, then according to the Cramér-Rao bound the QFI associated with estimating θ must be a factor of k^2 larger than the QFI associated with estimating $k\theta$. As such $Q_{\rm TM}(k) = k^2\,{\rm tr}(\hat{N}\varrho^{\rm in})\eta^k/(1-\eta^k)$. Finally, dividing by the number of lost photons gives: $Q_{\rm TM}(k) = k^2\eta^k/(1-\eta^k)^2$. $Q_{\rm SM}(k)$ can be found in the same way. These equations could be derived more formally by considering how the QFI transforms when multi-pass setups are used as is done in the main text for QFI per lost photon.

C: Gaussian details

Here we identify a Gaussian input state which maximizes the QFI related to the phase dependence of the displacement vector [31], noting that QFI related to the phase dependence of the $\mathbf{\Gamma}$ is not retrieved by homodyne measurements. Specifically it was found in Ref. [21] that homodyne measurements on squeezed thermal states are far from optimal. Following the definitions in the main text, the Gaussian input state $\varrho_{\rm G}^{\rm in}$ has a displacement vector $\boldsymbol{d}^{\rm in} = R(\varphi)(\alpha,0)^T$ and a covariance matrix:

$$\mathbf{\Gamma}^{\rm in} = \frac{1}{4}R(\varphi)\begin{pmatrix} {\rm e}^{2r} & 0 \\ 0 & {\rm e}^{-2r}\end{pmatrix}R^T(\varphi) \tag{14}$$

where $R(\varphi) = \begin{pmatrix}\cos\varphi & -\sin\varphi \\ \sin\varphi & \cos\varphi\end{pmatrix}$ is the usual rotation matrix. Following the lossy phase $\Lambda(\eta,\theta)$ the displacement vector of the output state, $\varrho_{\rm G}^{\rm out}$, is $\boldsymbol{d}^{\rm out} = R(\varphi+\theta)(\sqrt{\eta}\alpha,0)^T$ and the covariance matrix is:

$$\mathbf{\Gamma}^{\rm out} = \frac{1}{4}R(\varphi+\theta)\begin{pmatrix} {\rm e}^{2r}\eta+1-\eta & 0 \\ 0 & {\rm e}^{-2r}\eta+1-\eta\end{pmatrix}R^T(\varphi+\theta). \tag{15}$$

Loss introduces a factor of η into each covariance element and adds $(1-\eta)$ to the diagonal elements [21]. This can be thought of as introducing some vacuum noise from the environment mode (the reader should note that we use conventions to define Gaussian states and the covariance matrix in accordance with Ref.[29]). The states $\varrho_{\rm G}^{\rm in}$ and $\varrho_{\rm G}^{\rm out}$ are depicted in Fig. 4. The Fisher information from a normally distributed

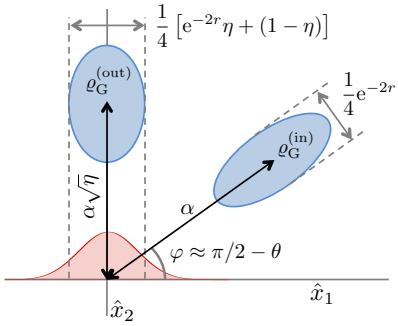

FIG. 4. Depiction of the covariances of the phase-squeezed Gaussian state discussed in the text. The homodyne signal is depicted along the horizontal axis.

measurement outcome x with a mean of μ and a variance of V about a parameter θ can be found using the definition of the Fisher information $\int\left[\frac{\partial}{\partial\theta}\ln p(x|\theta)\right]^2 p(x|\theta)dx$ [14]. This gives $F_x = \dot{\mu}^2/V + \dot{V}^2/(2V^2)$, where dots indicate derivatives with respect to the parameter to be estimated, such that we can insert the mean and variance of the homodyne signal upon measurement of $\varrho_{\rm G}^{\rm out}$, given by $d_1^{\rm out}$ and $\Gamma_{11}^{\rm out}$. We maximize the term in the Fisher information involving phase dependence of the displacement vector $(\dot{d}_1^{\rm out})^2/\Gamma_{11}^{\rm out}$ by setting $\varphi = \pi/2-\theta$ to obtain:

$$\begin{aligned} F_{\hat{x}}(\varrho_\theta)\big|_{\varphi=\pi/2-\theta} &= \frac{4\alpha^2\eta}{1+(e^{-2r}-1)\eta} \\ &= \frac{4\eta\,(n-n_{\rm sq})}{2\eta n_{\rm sq} - 2\eta\sqrt{n_{\rm sq}(n_{\rm sq}+1)}+1}. \end{aligned} \tag{16}$$

For a given mean number of photons, n, this has a maximum value when:

$$n_{\rm sq} = -\frac{\left(\sqrt{1-4(\eta-1)\eta n}-1\right)^2}{4(\eta-1)\left(\sqrt{1-4(\eta-1)\eta n}-\eta\right)} \tag{17}$$

and a Fisher information of:

$$2\eta\frac{1+2n(1-\eta)-\sqrt{1+4n(1-\eta)\eta}}{(\eta-1)^2}. \tag{18}$$

This expression could be used to compare this scheme to other schemes which are designed to operate in the extremely low photon number regime.

D: More general interferometers

We consider the interrogation of a SM lossy phase embedded in a setup, such that between each interrogation interference occurs between the outgoing mode from the phase and

another optical mode. Specifically we investigate an optical setup in which the coherent-state field amplitudes in two modes, $(\alpha,\beta)^T$ of the state $|\alpha\rangle|\beta\rangle$, are transformed by the matrix:

$$T=\left[\begin{pmatrix}1 & 0\\ 0 & \mathrm{e}^{\mathrm{i}k\theta+\phi}\eta^{k/2}\end{pmatrix}\begin{pmatrix}\cos(\xi/2) & -\sin(\xi/2)\\ \sin(\xi/2) & \cos(\xi/2)\end{pmatrix}\right]^h \quad (19)$$

where the right-hand matrix is an arbitrary-reflectivity beamsplitter and the left-hand matrix is the application of a control phase ϕ plus the phase and damping associated with the lossy phase $\Lambda^k(\eta,\theta)$. An optical setup which can implement this is shown in Fig. 3 of the main text. We performed a heuristic optimization of the QFI per lost photon produced by this strategy using the input state $|\alpha\rangle|0\rangle$ for a series of values of $\eta = 0.1, 0.2, ..., 0.9$ over the parameters h, k, ξ and $\varphi = k\theta + \phi$ whilst constraining k and h to be integers. in order to remove the effects of restricting to discrete k, we performed an optimization of $\ln^2\eta\, F'(\varrho)$, which we previously found to be of the form $f(\varphi,\gamma = \eta^k)$, and varied (h,φ,ξ) and γ. This yielded a classical strategy for which $F'(\varrho_{\mathrm{Cl}}) = 4\times 0.94/\ln^2\eta$. The reduction in RMSE per incident photon, afforded by non-classical techniques, was found to be 3.6% on average for $\eta = 0.1, 0.2, ..., 0.9$ and 3.0% when k was permitted to be non-integer. individual results are plotted in Fig. 2a) of the main text. Optimization details can be found in appendix E, and as the optimizations are not exhaustive there may be further room for improvement. Using additional reference beams, the same improvement can be made for TM phase estimation (as discussed in appendix F).

E: Optimization details

Given the two-mode coherent state input: $|\psi_{\mathrm{Cl}}^{\mathrm{in}}\rangle = |\alpha_1^{\mathrm{in}}\rangle|0\rangle$, where $\alpha_1^{\mathrm{in}} \in \mathbb{R}_{>0}$ without loss of generality, the output state after the network described by the transfer matrix T, given in Eq. (19), will be a two-mode coherent state $|\psi_{\mathrm{Cl}}^{\mathrm{out}}\rangle = |\alpha_1^{\mathrm{in}}T_{11}(\theta)\rangle|\alpha_1^{\mathrm{in}}T_{21}(\theta)\rangle$ which has a QFI of:

$$4\left(\alpha_1^{\mathrm{in}}\right)^2\left(\left|\frac{\partial T_{11}}{\partial\theta}\right|^2+\left|\frac{\partial T_{21}}{\partial\theta}\right|^2\right). \quad (20)$$

where T_{11} and T_{21} are matrix elements in the first column of T. This can be seen from the results in Ref. [31] and using the fact that QFI of a system is additive over separable subsystems. Alternatively this can be computed directly from the definition of the QFI. Therefore, the QFI per lost photon of $|\psi_{\mathrm{Cl}}^{\mathrm{out}}\rangle$ is

$$4\frac{\left|\frac{\partial T_{11}}{\partial\theta}\right|^2+\left|\frac{\partial T_{21}}{\partial\theta}\right|^2}{1-|T_{11}|^2-|T_{21}|^2}. \quad (21)$$

This expression was heuristically optimized. Through preliminary optimizations it was noticed that $\varphi = 0$ and $k = 1$ were generally the best values for these parameters. Then we numerically optimized over $\xi \in (0.1/h, 6/h)$ and $h \in \mathbb{N} = \{1, 2, \ldots\}$ whilst fixing $\phi = 0$ and $k = 1$ for each value of $\eta \in \{0.1, 0.2, \ldots 0.9\}$ using a standard numerical optimization package. ξ was restricted to be greater than $0.1/h$ to improve numerical stability. The results of these optimizations are shown in Table I.

η (set)	h (varied)	$h\xi$ (varied)	F'/Q'_{SM}
0.1	1	NA	0.900000
0.2	2	0.0100001	0.927824
0.3	3	0.0100005	0.922368
0.4	3	0.0100004	0.924007
0.5	5	0.0100000	0.930968
0.6	6	0.0100009	0.933002
0.7	9	0.0100000	0.934944
0.8	15	0.0100001	0.935805
0.9	32	0.0100076	0.936049

TABLE I. Optimized values of F' for a set of η. The values quoted have been rounded to six significant figures where appropriate.

The results shown in Table I appear to indicate that the best strategy always has a small $h\xi$ independent of η. However, as stated in Appendix D it is necessary to address the effects of confining this strategy to discrete numbers of interrogations. We performed a numerical optimization of $\ln^2\eta\, F'(\varrho)$, which we previously found to be of the form $f(\varphi,\gamma=\eta^k)$, by varying the optical setup (h,ξ) and γ. φ was again set to zero. The result of this optimization is shown in Table II. This result indicates that when η is close to one, a strategy which has a small $h\xi$ is not optimal.

γ (varied)	h (varied)	$h\xi$ (varied)	$F'/\lim_{k\to 0}Q'_{\mathrm{SM}}(k)$
0.988747	510	5.12423	0.940333

TABLE II. Optimized values of F' normalized to the quantum limit $\lim_{k\to 0}Q'_{\mathrm{SM}}(k)$. The values quoted have been rounded to six significant figures where appropriate.

F: General networks for two-mode phase estimation

We were unable to find schemes for TM phase estimation which went above the optimal classical MP F', given in Eq. (4) of the main text, without using any reference beams. However, we note that the phase difference between the two modes $\theta_\delta = \theta_1 - \theta_2$, with equally lossy and uncorrelated

phases in each mode θ_1 and θ_2, could be measured by separately interrogating the phase in each arm, and utilizing two additional modes to perform the measurement following the SM strategies.

Measuring each phase, θ_1 and θ_2, equally precisely will require twice as many photons to be lost in comparison with the measurement of a single phase to the same precision. The RMSE of the phase difference will be twice as big as it is for each phase θ_1 and θ_2 since $\Delta^2\theta_\delta = \Delta^2\theta_1 + \Delta^2\theta_2$ [32]. Therefore, this procedure would provide one quarter of the Fisher information per lost photon about the phase difference as in the case of SM phase estimation. Hence the ratio between optimal quantum and this classical strategy for TM phase estimation, when reference beams are used, would be as for SM phase estimation in the main text.

G: Experimental imperfections

To understand how deviations from the ideal case affect the scope for quantum enhancement in a multi-pass setup we consider optical loss $1-\eta_p$ encountered before incidence upon the lossy-phase $\Lambda(\eta,\theta)$, round-trip loss $1-\eta_r$ encountered between applications of $\Lambda(\eta,\theta)$ and measurement loss $1-\eta_m$ encountered after the last application of $\Lambda(\eta,\theta)$. Thus, for k passes the total transmissivity is $\eta_{\text{tot}} = \eta^k\eta_p\eta_m\eta_r^{k-1}$ and the number of photons lost via the lossy-phase is:

$$\begin{aligned}\langle\hat{n}_l\rangle &= \sum_{i=1}^{k}(1-\eta)\eta_p\,\mathrm{tr}(\hat{N}\varrho^{\text{in}})\eta_r^{i-1}\eta^{i-1} \\ &= \mathrm{tr}(\hat{N}\varrho^{\text{in}})\eta_p(1-\eta)(1-\eta^k\eta_r^k)\big/(1-\eta\eta_r)\end{aligned} \tag{22}$$

which has been found by summing over the number of scattered photons each time the state is incident upon the lossy-phase. With these additional losses, we consider the resource to be the QFI per photon lost via the lossy phase (which is equivalent to considering the QFI per photon incident on the lossy phase since the number lost via the phase is proportional to the number incident upon the phase).

When these additional losses are included we were unable to find general closed form expressions for the optimal number of passes for either classical or quantum strategies. Because of this we could not compute expressions for optimal QFI using quantum or classical states with imperfect multi-pass strategies. However, using numerical methods, we were able to clarify situations for which quantum strategies grant precision gains which are larger than 20% (i.e. larger than in the ideal case). We focused on evaluating the difference in achievable precision between a quantum strategy and an equivalent classical strategy, i.e. with the same losses. It should be noted that the advantage granted here by quantum techniques is not fundamental, in the sense that it could only be achieved by non-classical techniques, since better components could improve the classical strategy.

For a given input state the QFI obtainable from a multi-pass scheme is dependent on the total phase shift applied and on the overall transmissivity, both of which can be found from $k, \eta_p\eta_m, \eta$ and η_r. The number of photons lost via the phase is a function of the form $\eta_p \times \mathrm{tr}(\hat{N}\varrho^{\text{in}}) \times q(k,\eta,\eta_r)$ where $q(k,\eta,\eta_r) = (1-\eta)(1-\eta^k\eta_r^k)\big/(1-\eta\eta_r)$. Therefore, in the case that the QFI for a given input state is proportional to the number of photons it contains, as is the case for both the optimal quantum state and the optimal classical state, the QFI per photon lost via the phase is a function of the form $(1/\eta_p) \times z(\eta_p\eta_m, k, \eta, \eta_r)$. Therefore, the ratio between the achievable precisions using quantum and classical states is independent of η_p once the product $\eta_p\eta_m$ is specified. Furthermore, the two different optimal number of passes $k_{\text{opt}}^{\text{Cl}}$ and $k_{\text{opt}}^{\text{Q}}$ for classical or quantum MP strategies are determined by the rest of the parameters. Because of this, we can investigate the ratio of achievable precisions using optimal quantum and classical states in multi-pass schemes as a function of only η, η_r and $\eta_p\eta_m$. This ratio is the same for both SM and TM phase estimation because the information gained differs by a factor of four for both the classical and quantum strategies.

To establish if considering additional losses made the quantum strategy more or less advantageous relative to a classical strategy we sought to find which combinations of η, η_r and $\eta_p\eta_m$ lead to a greater quantum advantage than in the ideal case. For a grid of 150×150 values of $(\eta_r, \eta_p\eta_m)$ we tried to find the highest value of η_r such that the quantum strategy provided a reduction in RMSE of more than 20%. This identifies a region of the parameter space within which it may be possible to achieve a reduction in RMSE of more than 20%. Our method for finding the highest η_r, for each combination of $(\eta_r, \eta_p\eta_m)$, was (starting with $\eta_r = 1$):

1. Optimize the number of passes for the classical and then the quantum strategies.
2. Then calculate the quantum advantage.
3. Iterate 1. and 2. for decreasing values of η_r until the advantage becomes greater than a 20% reduction in RMSE.

The highest η_r required was determined to a precision of ± 0.00008. A surface of these values for η_r are plotted in Fig. 5.

From these optimizations we note that a qualitative change to the quantum strategies occurs when additional losses were included: The optimal number of passes $k_{\text{opt}}^{\text{Q}}$ is not always one as it is in the ideal case. This means that imperfect quantum strategies can also make use of multi-pass techniques. As can be seen in this plot, the resultant surface appears to be approximately $\eta_r = \eta_p\eta_m$ where it is present. in fact, the surface lies below $\eta_r = \eta_p\eta_m$ at all points meaning that for all the 22500 values of η_r and $\eta_p\eta_m$ we studied: in order to obtain a reduction in RMSE of more than 20% the individual round-trip loss $1-\eta_r$ must be greater than the combined state preparation and measurement loss $1-\eta_p\eta_m$. in places the surface is missing which means there was no value of η_r for which quantum techniques granted a reduction in RMSE of more than 20%.

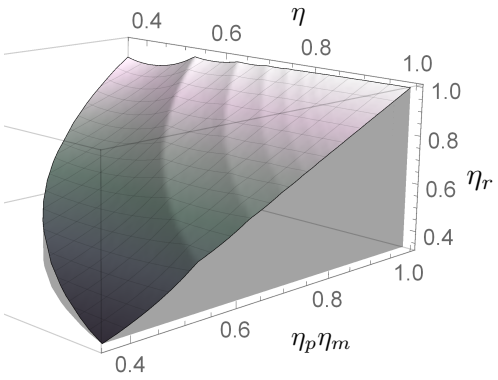

FIG. 5. Plot showing which combinations of parameters η, η_r and $\eta_p\eta_m$ can lead to a quantum advantage greater than that of the ideal case. The shaded gray region below the plotted surface is the region which allows a quantum advantage that reduces the RMSE by more than 20% over a comparable classical strategy. Bumps in the surface correspond to the classical or quantum strategies considered with different optimal numbers of passes.

This will occur when it is not necessary to use more than one passage through the phase since in this case the round-trip loss will not play a role.

We have not studied the effects of imperfections in the more general optical setups of Appendix D and F. We expect that the efficacy of these setups to be more heavily degraded by component imperfection and will only offer an advantage when the sample introduces the dominant source of loss. We do report one observation about the general setups: The QFI obtained using the setups specified in Table I is almost entirely ($\geq 99\%$) in the mode containing the lossy phase. Therefore, we would not expect losses in the reference mode to significantly reduce the efficacy the setups specified in Table I.